Stereospecific Polymerization of Methyl Methacrylate with Single-Component Zirconocene Complexes: Control of Stereospecificity via Catalyst Symmetry

Holger Frauenrath, Helmut Keul, and Hartwig Höcker*

Institut für Technische Chemie und Makromolekulare Chemie der RWTH Aachen, Worringer Weg 1, 52056 Aachen, Germany

Received July 18, 2000; Revised Manuscript Received October 24, 2000

ABSTRACT: We report the stereospecific polymerization of methyl methacrylate (MMA) with single-component cationic zirconocene catalysts. The complexes $Me_2CCpIndZrMe(thf)^+BPh_4^-$ (**1**) and $Me_2CCp_2ZrMe(thf)^+BPh_4^-$ (**2**) are active catalysts for the polymerization of MMA, in remarkable contrast to other cationic zirconocenes. While **1** yields highly isotactic poly(methyl methacrylate) (PMMA), **2** is syndiospecific at low temperatures. This is the first example for a rational control of PMMA microstructure via catalyst symmetry. Polymerization kinetics and stereospecificity control in MMA polymerization with **1** and **2** are discussed. On the basis of the experimental data, a possible polymerization mechanism is proposed.

Introduction

Since the beginning of the 1980s the use of metallocenes as polymerization catalysts has developed from a model system for Ziegler−Natta catalysis to a field of major academic and industrial interest.[1] The *ansa*-zirconocenes first described by Brintzinger et al.[2] are striking examples for the understanding of structure−reactivity relationships in chemistry. Thus, different geometric and electronic properties of various bridged ligands allow for the control of catalyst activity, molecular weight, polymer microstructure, or comonomer content and distribution. With this "tool chest" completely new materials have successfully been designed. Encouraged by the detailed understanding of zirconocene catalyst systems, many other transition metal complexes have been studied concerning their polymerization activity.[3] However, one important goal has not been achieved yet. That is the copolymerization with functionalized olefins which would pave the way for the next generation of even more complex, functional materials on the basis of polyolefins. A first step on this way would be the control of stereochemistry by the nature of the catalyst in the catalytic polymerization of functional olefins such as MMA. Thus, syndiotactic PMMA would combine properties typical for PMMA with enhanced mechanical and thermal stability. Potential catalysts for the formation of polyolefin−PMMA block copolymers must allow for efficient polymerization and stereocontrol of MMA and olefin polymerization as do the zirconocene catalysts in olefin polymerization today.

In 1992 Collins et al. described the polymerization of MMA catalyzed by zirconocenes.[4] Application of a two-component catalyst system consisting of the cationic complex $Cp_2ZrMe(thf)^+BPh_4^-$ and the neutral ester enolate complex $Cp_2ZrMe\{OC(OR)CMe_2\}$ accomplishes polymerization of MMA via a Michael addition mechanism. The polymerization mechanism is incompatible with the insertion mechanism in olefin polymerization, but it should at least allow for studying the relationship of catalyst geometry and polymer microstructure. Although the application of chiral *ansa*-zirconocenes is mentioned in one paper,[4b] there has been no systematic study on this question so far. We have been able to show[5a] that catalyst systems consisting of chiral cationic and ester enolate complexes also yield basically atactic, syndio-enriched PMMA as do the achiral systems described by Collins et al.

Anionic polymerization of MMA is known to be stereospecific under certain reaction conditions, i.e., yielding 100% isotactic PMMA with *tert*-C_4H_9MgBr and 90% syndiotactic PMMA with *tert*-$C_4H_9Li/AlEt_3$ in toluene at −78 °C in both cases.[6] Yasuda et al. and Marks et al. successfully performed stereospecific MMA polymerizations applying samarocene catalysts.[7] Soga et al. describe the use of multicomponent zirconocene-based catalyst systems with a large excess of zinc alkyls for the isospecific polymerization of MMA.[8] Recently, Collins et al.[9] published the first stereospecific polymerization of MMA with a single-component zirconocene catalyst. Gibson et al.[10a] have studied MMA polymerization with various cationic zirconocenes, including $Me_2CCpIndZrMe^+MeB(C_6F_5)_3^-$, with respect to the activation method. Furthermore, Gibson et al.[10b] mention the synthesis of syndiotactic PMMA using an aluminum catalyst and a nickel cocatalyst at low temperatures.

Results and Discussion

The cationic complexes $Me_2CCpIndZrMe(thf)^+BPh_4^-$ (**1**) and $Me_2CCp_2ZrMe(thf)^+BPh_4^-$ (**2**) are highly active for the polymerization of MMA without the addition of the corresponding ester enolate complex, while other cationic complexes **3**−**6** that have been tested are not.[11] Typical results of MMA polymerization with the cationic complexes $Me_2CCpIndZrMe(thf)^+BPh_4^-$ (**1**) and $Me_2CCp_2ZrMe(thf)^+BPh_4^-$ (**2**) are shown in Tables 1 and 2.

MMA polymerization with **1** is highly isospecific, in remarkable contrast to MMA polymerization with a catalyst system consisting of **1** and **7**.[5] Polymerization with **2** yields syndiotactic PMMA at low temperatures. It can be stated that this is the first example of a correlation of PMMA microstructure and catalyst structure. The similar ligand structure of **1** and **2** generates an active zirconocene catalyst for MMA polymerization, while catalyst symmetry allows for the control of PMMA microstructure.

* Corresponding author. E-mail: hoecker@dwi.rwth-aachen.de.

10.1021/ma001251v CCC: $20.00
Published on Web 12/08/2000

Table 1. Typical Results of MMA Polymerization with $Me_2CCpIndZrMe(thf)^+BPh_4^-$ (1)[a]

T_p/°C	t_p/min	yield[b]/%	$\bar{M}_n$[c]	$\bar{M}_w/\bar{M}_n$[c]	$I^* = \bar{M}_{n,theor}/\bar{M}_{n,exp}$[d]	*mm*[e]/%	*mmmm*[f]/%
30	20	54	40 500	1.43	0.33	84.3	74.9
20	40	62	45 700	1.42	0.34	87.0	79.6
10	60	94	51 000	1.42	0.46	89.0	82.1
0	90	97	58 800	1.34	0.41	90.4	84.5
−10	180	97	55 100	1.30	0.44	92.1	87.6
−20	180	93	55 300	1.24	0.42	93.5	n. d.
−30	240	77	57 300	1.21	0.34	94.7	91.5

[a] Reaction conditions: [MMA] = 2 mol/L, [**1**] = 8 mmol/L; solvent CH_2Cl_2. [b] Determined gravimetically. [c] Determined by GPC relative to PMMA standards. [d] Catalyst efficiency I^* calculated from theoretical $M_{n,theor}$ = [MMA]/[Zr] × conversion. [e] Determined by ^{1}H NMR spectroscopy. [f] Determined by ^{13}C NMR spectroscopy.

Table 2. Typical Results of MMA Polymerization with $Me_2CCp_2Me(thf)^+BPh_4^-$ 2[a]

T_p/°C	t_p/min	yield[b]/%	$\bar{M}_n$[c]	$\bar{M}_w/\bar{M}_n$[c]	$I^* = \bar{M}_{n,theor}/\bar{M}_{n,exp}$[d]	*rr*[e]/%	*rrrr*[f]/%
30	20	65	66 600	1.64	0.12	69.0	52.1
20	30	61	93 000	1.60	0.08	72.9	57.6
10	40	59	104 100	1.38	0.07	75.1	59.2
0	60	81	90 600	1.32	0.11	78.8	61.9
−10	105	86	123 200	1.30	0.09	80.1	67.2
−20	180	71	110 500	1.35	0.08	82.4	69.1
−45	1080	98	78 500	1.31	0.16	89.0	76.9

[a] Reaction conditions: [MMA] = 2 mol/L, [**1**] = 16 mmol/L; solvent CH_2Cl_2. [b] Determined gravimetically. [c] Determined by GPC relative to PMMA standards. [d] Catalyst efficiency I^* calculated from theoretical $M_{n,theor}$ = [MMA]/[Zr] × conversion. [e] Determined by ^{1}H NMR spectroscopy. [f] Determined by ^{13}C NMR spectroscopy.

Polymerization Kinetics. Figure 1 shows plots of the MMA conversion versus polymerization time in a first-order plot with $Me_2CCpIndZrMe(thf)^+BPh_4^-$ (**1**) as a catalyst at different polymerization temperatures. Quantitative yields are only achieved at polymerization temperatures of 0 °C and below. Above 0 °C the polymerization reaction appears to be terminated within a couple of minutes. At lower temperatures the polymerization reaction can be driven to completion, and the dependence of monomer conversion on polymerization time approaches to what should be expected for first-order kinetics. At the same time, a short initiation period is observed. Apparently, the cationic complex **1** itself is not the active species.

A plot of the molecular weights vs MMA conversion in Figure 2 reveals a linear dependence up to high conversions, especially at low polymerization temperatures. This indicates the absence of a chain transfer reaction. The experimentally determined number-average molecular weights are substantially higher than the theoretical molecular weights determined by the ratio of monomer and initiator concentration, if one assumes a living polymerization. Consequently, catalyst efficiencies I^* determined from the ratio of experimental and theoretical number-average molecular weight are below 1 (Tables 1 and 2). Either the active species is not generated in a monomolecular reaction from **1** and **2**, or just part of the zirconocene species is active. The latter explanation is more straightforward if one considers the results of reaction kinetics. In the case of **2**, catalyst efficiences are even lower, and no polymerization is observed for catalyst concentrations below 12×10^{-3} mol/L. In CD_2Cl_2 decomposition of **2** occurs within a couple of minutes. This may point to the fact that part of the zirconocene species is decomposed already before it is transformed into the active species.

Molecular weight distribution of PMMA broadens progressively with increasing MMA conversion (Figure 3). Molecular weight distributions of PMMA are moderately narrow for polymerization temperatures above 0 °C with polydispersities below 1.2 only for moderate monomer conversion at low polymerization temperatures.

Chart 1

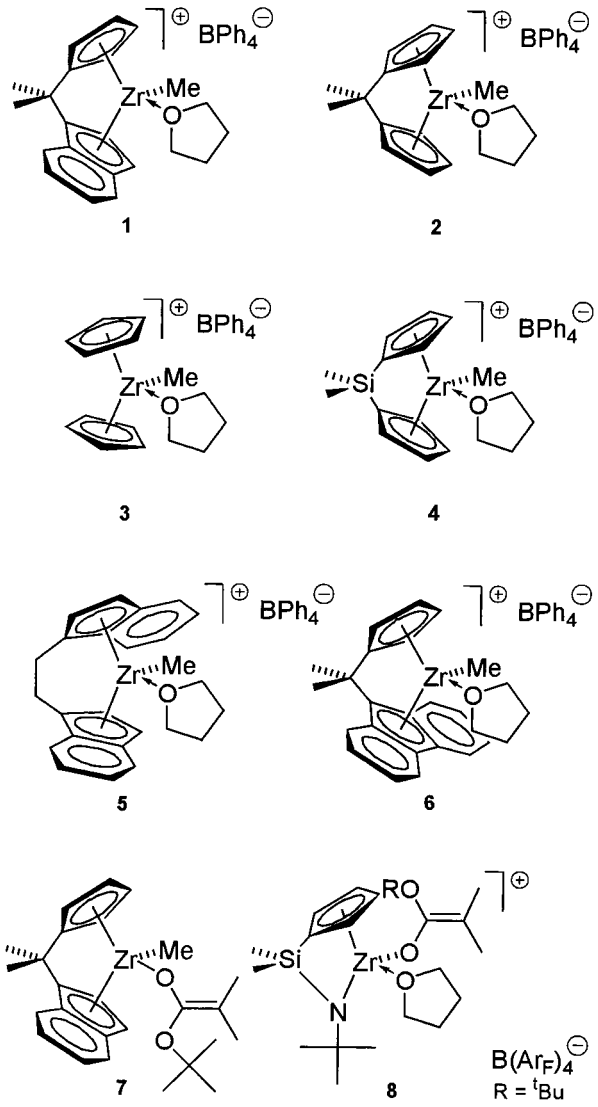

The graphs shown in Figure 1 are successfully fitted with an equation derived from a kinetic model that

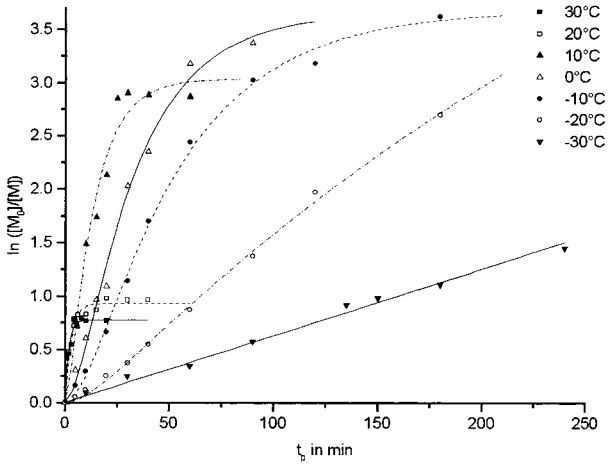

Figure 1. Kinetics of MMA polymerization with **1** at different polymerization temperatures; lines from function fitting.

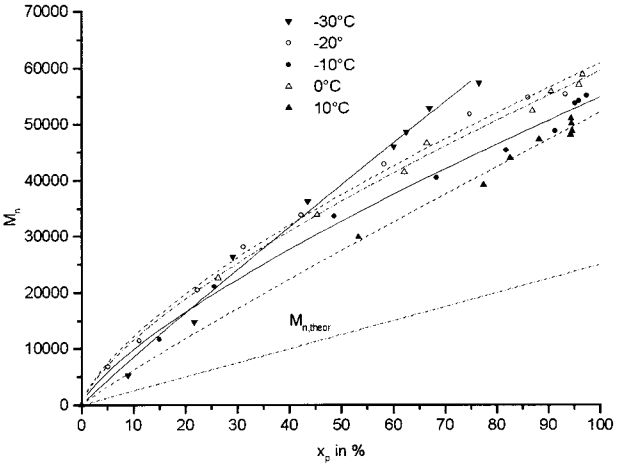

Figure 2. Plot of number-average molecular weight vs monomer conversion in MMA polymerization with **1** at different polymerization temperatures; dashed line represents theoretical molecular weight $M_{n,theor}$ = [MMA]/[Zr] × conversion.

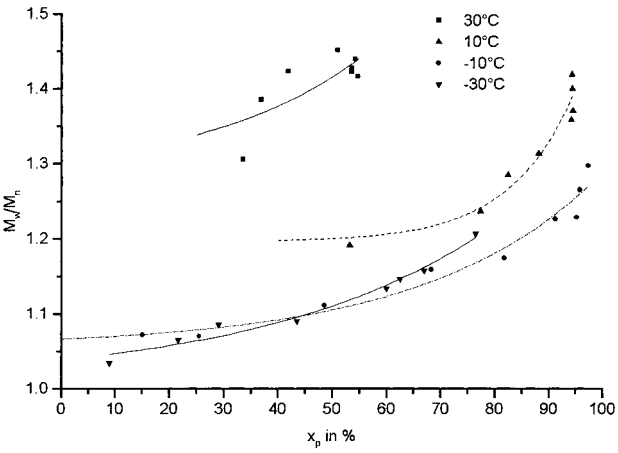

Figure 3. Polydispersities of PMMA polymerized with **1** as a function of monomer conversion at different polymerization temperatures.

assumes first-order kinetics with respect to MMA with time-dependent catalyst concentrations, taking into account an initiation reaction and a termination reaction (monomer concentration $[M]_t$, initial monomer concentration $[M]_0$, concentration of active species $[Zr^*]_t$, initial zirconocene concentration $[Zr]_0$, rate constants of

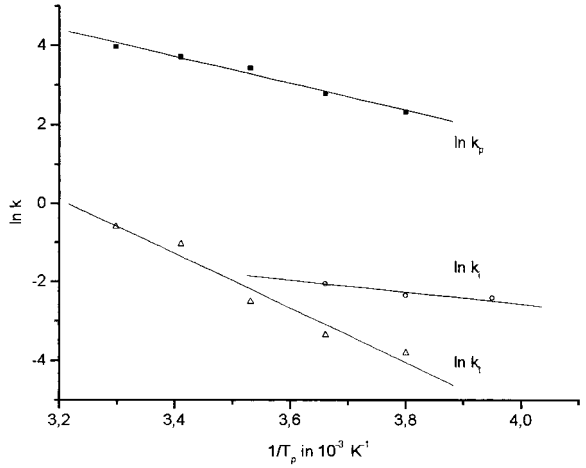

Figure 4. Eyring plot of the rate constants of propagation k_p, of initiation k_i, and of termination k_t at different polymerization temperatures determined by function fitting of the experimental kinetic data.

propagation k_p, of initiation k_i, and of termination k_t):

$$-\frac{d[M]_t}{dt} = k_p[M]_t[Zr^*]_t$$

$$-\frac{d[M]_t}{dt} = k_p[M]_t[Zr]_0\frac{k_i}{k_t - k_i}(e^{-k_i t} - e^{-k_t t})$$

$$\ln\frac{[M]_0}{[M]_t} = k_p[Zr]_0\frac{k_i}{k_t - k_i}\left\{\frac{1}{k_t}(e^{-k_t t} - 1) - \frac{1}{k_i}(e^{-k_i t} - 1)\right\}$$

The activation energies of the propagation, the initiation, and the termination reaction are obtained from an Eyring plot of the respective rate constants derived from the fitting of the experimental data (Figure 4). The activation energies are $E_{a,p} = 28 \pm 2.3$ kJ/mol for the propagation reaction, $E_{a,i} = 13 \pm 8.9$ kJ/mol for the initiation reaction, and $E_{a,t} = 57 \pm 6.9$ kJ/mol for the termination reaction.

Control of Stereospecificity. As seen from Tables 1 and 2, MMA polymerization with $Me_2CCpIndZrMe(thf)^+BPh_4^-$ **(1)** is highly isospecific already at room temperature, whereas MMA polymerization with $Me_2CCp_2ZrMe(thf)^+BPh_4^-$ **(2)** is syndiospecific at low temperatures. From the Eyring plots of the relative diad abundances (calculated from the triad abundances determined by ^{1}H NMR spectroscopy) at different polymerization temperatures (Figure 5), the differences of activation energies that control the stereospecificity is estimated to be $E_{a,r} - E_{a,m} = 12.2 \pm 0.6$ kJ/mol in the case of **1** and $E_{a,r} - E_{a,m} = -9.5 \pm 0.4$ kJ/mol in the case of **2**.

Pentad analysis of the polymers obtained is consistent with an enantiomorphic site mechanism in the case of **1**, with a ratio *mmmr*:*mmrr*:*mrrm* ≈ 2:2:1 in the whole temperature range (Figure 6). Other error pentads are practically absent; only at 30 °C is a measurable amount of *mrmm* detected. The syndiospecificity of **2** appears to be due to chain end control, consistent with a ratio *rrrm*:*rrmr* ≈ 2:1 in the whole temperature range (Figure 7).

Proposal for a Polymerization Mechanism. To explain the experimental results, we propose the mechanism displayed in Scheme 1 as a working hypothesis. This mechanism is basically identical to the mechanism

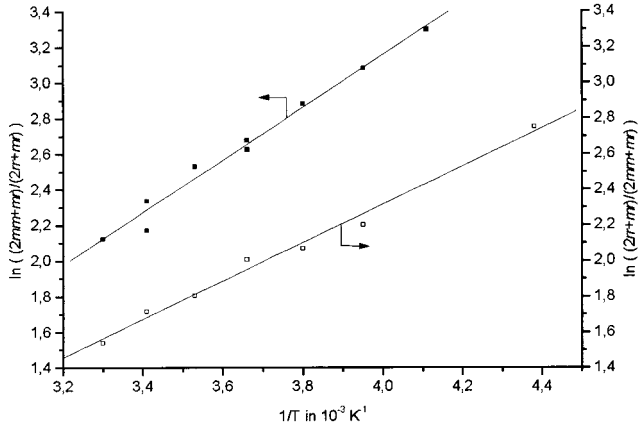

Figure 5. Eyring plot of the relative diad abundance in PMMA polymerized with **1** (■) and **2** (□), calculated from triad abundances determined by ^{1}H NMR spectroscopy.

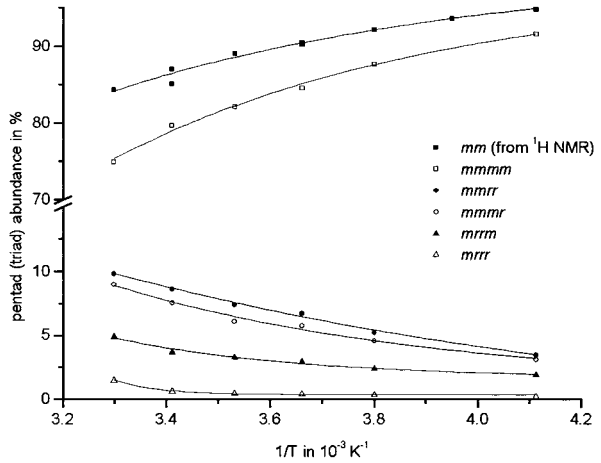

Figure 6. Pentad (triad) abundances in PMMA polymerized with **1** at different polymerization temperatures, determined by ^{13}C NMR (^{1}H NMR) spectroscopy.

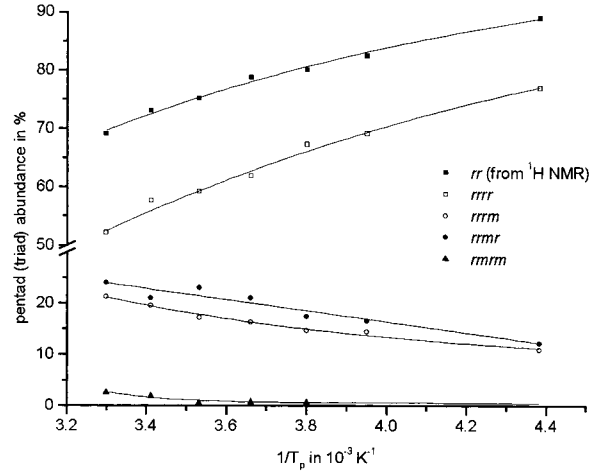

Figure 7. Pentad (triad) abundances in PMMA polymerized with **2** at different polymerization temperatures, determined by ^{13}C NMR (^{1}H NMR) spectroscopy.

that was found for MMA polymerization with the isoelectronic samarocenes by Yasuda et al.[7a]

The observed initiation period is due to the transfer of a methyl group of a zirconocenium cation to a coordinated MMA molecule. The resulting cationic ester enolate complex is the active species in the polymerization reaction. It combines the functions of the two catalyst components in Collins-type MMA polymerizations. It activates the growing chain end as a donor and at the same time an incoming MMA molecule as an acceptor. The possibility of such a monometallic mechanism has been evaluated in calculations by Sustmann et al.[12] It was found to be only slightly more unfeasable compared to a bimetallic mechanism. Our proposal is further supported by the recent findings of Collins et al.,[9] who describe the isospecific polymerization of MMA with the cationic ester enolate complex **8**.

So why are **1** and **2** active while **3**−**6** are not? One remarkable feature of **1** and **2** is the large ligand aperture with a Cp−Zr−Cp angle of only 116.6° (in $Me_2CCp_2ZrCl_2$,[13a] to be compared with 129.3° in Cp_2ZrCl_2[13b] and 125.4° in $Me_2SiCp_2ZrCl_2$[13c]) caused by the very short isopropylidene bridge. This geometric feature or the electronic properties inevitably connected with it may alter reactivity, i.e., allow for the transfer of the methyl group or the formation of the cyclic intermediat. Gibson et al.[10a] find different dimethylzirconocenes also being active for MMA polymerization when activated with $B(C_6F_5)_3$. This may point to the fact that their method of activation is superior, activating also complexes that are less prone to polymerizing MMA.

How can the stereospecificity of **1** and **2** be explained? **1** is a C_1-symmetric complex with two substantially different coordination sites at the zirconium center. That is to say, one side of the complex does not place any constraint on either the conformation of the growing chain or the orientation of an incoming MMA molecule while the other one does. It must be assumed that the isospecificity of **1** is the result of the polymerization step always taking place on the same side of the catalyst. Consequently, after each polymerization step a fast active site epimerization reaction would occur, i.e., in an associative mechanism with the assistance of a solvent molecule or MMA as proposed by Collins et al.[9] The driving force into one certain position could be the preference of the bulky polymer chain for the side without steric hindrance. As a result, MMA polymerization with **1** would appear to be isospecific with enantiomorphic site control. In the case of **2** the two coordination sites are equivalent. No preference for either one should be observed, giving room for a chain end control mechanism due to the cyclic intermediate. Consequently, **2** should yield basically atactic PMMA with growing syndiotacticity at lower temperatures, when active site epimerization is slowed down.

The low catalyst efficiences have already been explained in terms of a reduction of the concentration of the active species by the initiation and the termination reaction. As the proposed mechanism is a working hypothesis, it is of course also possible that it proceeds via a bimetallic pathway like it was discussed by Yasuda et al.[7f] and Gibson et al.[10a]

Conclusions. We have been able to show that the cationic complexes $Me_2CCpIndZrMe(thf)^+BPh_4^-$ (**1**) and $Me_2CCp_2ZrMe(thf)^+BPh_4^-$ (**2**) are highly active for MMA polymerization, in remarkable contrast to many other cationic zirconocenes. With isotactic PMMA derived from **1** and syndiotactic PMMA derived from **2** we have found the first example of a rational control of PMMA microstructure via catalyst structure. The experimental results can be explained in terms of mechanistic considerations already discussed in the literature and are consistent with similar findings of other groups. This mechanism still has to be proved, and the nature of the

Scheme 1. Proposal for a Polymerization Mechanism in MMA Polymerization with 1 and 2

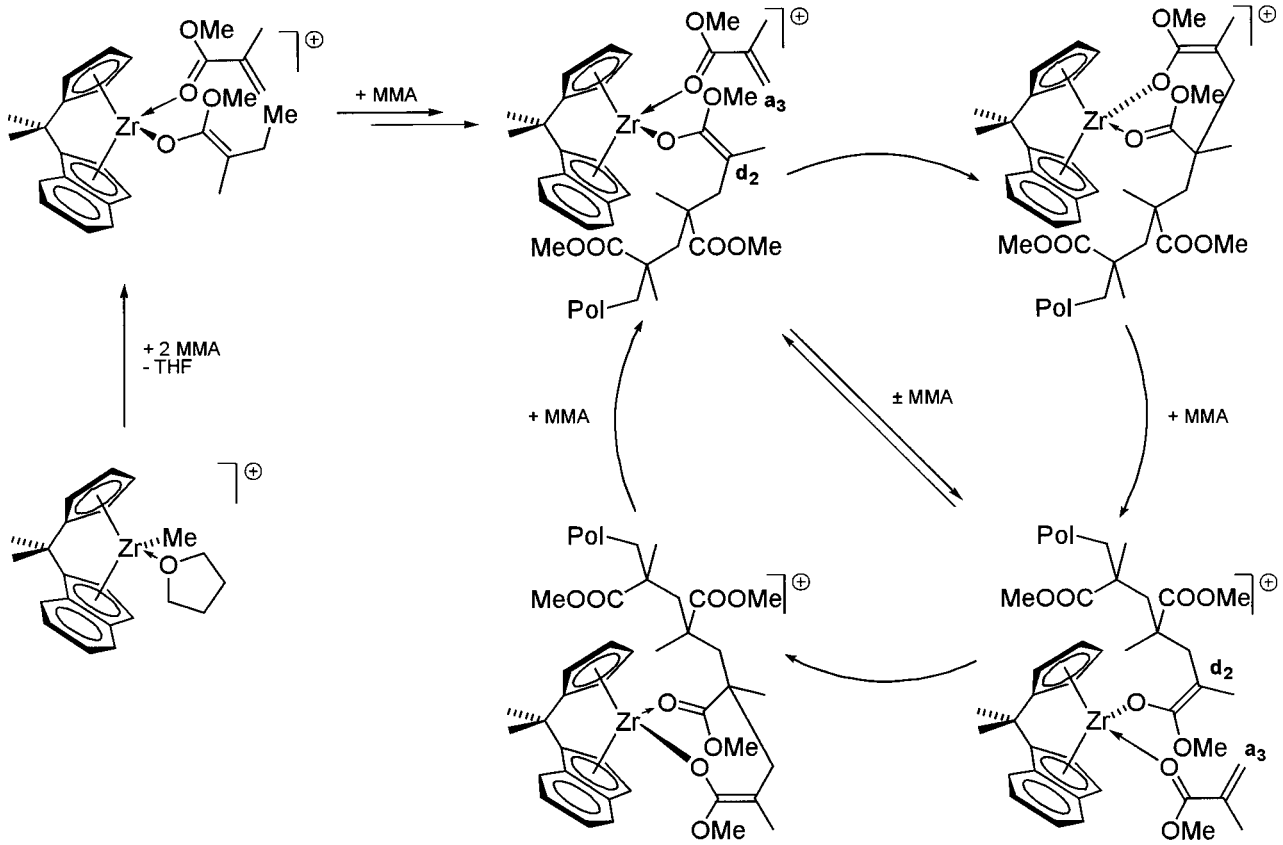

termination reaction has to be examined. Experiments concerning the role of the solvent, the reaction order with respect to the catalyst, and the nature of the initiator as well as end group analyses are in progress.

Experimental Section

General Procedures. All experiments were carried out in a nitrogen atmosphere using standard Schlenk techniques. Nitrogen was passed over an activated copper catalyst (BASF R3-11), molecular sieves, and K/Al_2O_3 for purification. Me_3SiCl (Fluka, >99%), MeLi (Fluka, 1.6 M solution in DE), BuLi (Aldrich, 2 M solution in pentane), $NaBPh_4$ (Fluka, >98%), and $ZrCl_4$ (Fluka) were used without further purification. All other chemicals were purified using the standard methods. $[HNBu_3][BPh_4]$,[14] $Zr(NEt_2)_4$[5], $Me_2C(Cp)(Ind)ZrCl_2$[5], $Me_2C(Cp)(Ind)ZrMe_2$,[5] and $[Me_2C(Cp)(Ind)Zr(Me)(thf)][BPh_4]$ (**1**)[5] as well as the cationic zirconocene complexes **3**−**6**[11] were prepared according to published procedures. Toluene and THF were dried over sodium/benzophenone, and CH_2Cl_2 was dried over P_2O_5. All solvents were stored in a nitrogen atmosphere. MMA was stored at 0 °C over CaH_2 and freshly distilled before use. All deuterated solvents were degassed and stored over molecular sieves (4 Å).

All ^1H and ^{13}C NMR spectra were recorded on a Bruker DPX 300 FT-NMR spectrometer at 300 and 75 MHz, respectively. All chemical shifts are given in ppm with tetramethylsilane as a reference. Quantitative ^{13}C spectra for the anlysis of PMMA microstructure were recorded with at least 16 000 scans using an inverse gated decoupling pulse sequence.

All gel permeation chromatography (GPC) analyses were carried out at room temperature using a HPLC pump (Waters 510) and a refractive index detector. The eluent was THF stabilized with 250 mg/mL 2,6-di-*tert*-butyl-4-methylphenol. The flow rate was 1.0 mL/min. Four columns were applied (PS-DVB gels from MZ Analysentechnik), with pore sizes of 100, 100, 1000, and 10 000 Å. Number-average molecular weights and polydispersities of PMMA are given relative to PMMA standards.

Synthesis of $Me_2CCp_2ZrCl_2$. To a solution of 10.6 g (28 mmol) of $Zr(NEt_2)_4$ in 80 mL of toluene a solution of 4.8 g (28 mmol) of $Me_2C(CpH)_2$ in 30 mL of toluene was slowly added via a double-tipped needle at −78 °C. The solution was allowed to warm to room temperature and stirred for 12 h. It was then heated to 90 °C under stirring for 72 h. Toluene and other volatile components were removed in vacuo, and the mixture was then again diluted with 50 mL of toluene. 9 g (83 mmol) of Me_3SiCl was added slowly at 0 °C, and the mixture was stirred for 24 h at room temperature. Filtering off the precipitated light yellow powder and washing with hexane yielded 7.85 g (84%). ^1H NMR ($CDCl_3$): δ 1.75 (s, 6H, CMe), 5.70 (m, 4H, Cp), 6.61 (m, 4H, Cp). ^{13}C NMR ($CDCl_3$): 23.0 (CMe_2), 36.7 (CMe_2), 102.0, 105.8, 121.8 (Cp).

Synthesis of $Me_2CCp_2ZrMe_2$. 11 mL of MeLi solution (1.8 M in DE) was added slowly at 0 °C to a suspension of 3.31 g (10 mmol) of $Me_2CCp_2ZrCl_2$ in 60 mL of DE. The mixture was stirred for 2 h at 0 °C and for 12 h at room temperature. The volatiles were removed in vacuo. The residue was treated with 50 mL of toluene. Filtration and removal of the toluene in vacuo yielded 2.51 g (86%) of a light brown powder. ^1H NMR ($CDCl_3$): δ −0.23 (s, 6H, ZrMe), 1.62 (s, 6H, CMe), 5.59 (m, 4H, Cp), 6.65 (m, 4H, Cp). ^{13}C NMR ($CDCl_3$): 22.9 (CMe_2), 27.3 (ZrMe), 35.6 (CMe_2), 103.7, 113.7, 123.3 (Cp).

Synthesis of $[Me_2CCp_2Zr(Me)(thf)]^+[BPh_4]^-$. 3.87 g (7.66 mmol) of $[HNBu_3]^+[BPh_4]^-$ was suspended in 80 mL of toluene. Under vigorous stirring a solution of 2.28 g (7.82 mmol) of $Me_2C(Cp)(Ind)ZrMe_2$ in 20 mL of THF was added slowly via a double-tipped needle. The mixture was stirred for 2 h at room temperature, and toluene was removed from the light brown precipitate that had been formed via a cannula. The solid residue was dried in vacuo, leaving 3.57 g (67%) of a light yellow solid. ^1H NMR (CD_2Cl_2): δ 0.45 (s, 3H, ZrMe), 1.32−1.95 (m, 10H, THF and CMe_2), 3.40 (br s, 4H, THF), 5.23−6.38 (m, 8H, Cp), 6.84 (m, 4H, BPh_4), 6.98 (m, 8H, BPh_4), 7.29 (m, 8H, BPh_4). ^{13}C NMR (CD_2Cl_2): 26.5 (THF), 22.2 and 28.3 (CMe_2), 40.4 (CMe_2), 44.3 (ZrMe), 78.8 (THF), 108.3, 112.2, 119.4, 131.9, 130.6 (Cp), 124.6, 128.4, 138.6, 166.5 (BPh_4).

MMA Polymerizations. 2.5 g (25 mmol) of MMA and 7.5 mL of CH_2Cl_2 containing approximately 3% (w/w) hexylbenzene were placed in a 50 mL Schlenk tube with a septum and stirred at the desired polymerization temperature for 30 min. The polymerization was started by addition of a solution of the catalyst in 2.5 mL of CH_2Cl_2. In the kinetic experiments samples of approximately 0.05 mL were taken from the reaction mixture. Relative polymer yield was determined by GPC via integration of the polymer peaks relative to hexylbenzene as an internal standard. Absolute polymer yield was determined gravimetically by terminating the reaction just after taking off the last sample by addition of 2 mL of MeOH/HCl(aq)/hydroquinone (90/9.9/0.1% w/w), precipitation of PMMA in MeOH, filtration, and drying in vacuo.

References and Notes

(1) (a) Brintzinger, H.-H.; Fischer, D.; Mühlhaupt, R.; Rieger, B.; Waymouth, R. *Angew. Chem.* **1995**, *107*, 1255−1283. (b) Balsam, M.; Barghoorn, P.; Stebani, U. *Angew. Makromol. Chem.* **1999**, *267*, 1−9.

(2) (a) Wild, F. R. W. P.; Wasiucionek, M.; Huttner, G.; Brintzinger, H.-H. *J. Organomet. Chem.* **1985**, *288*, 63−67. (b) Kaminsky, W.; Külper, K.; Brintzinger, H.-H.; Wild, F. R. W. P. *Angew. Chem.* **1985**, *97*, 507−508.

(3) Britovsek, G. J. P.; Gibson, V. C.; Wass, D. F. *Angew. Chem.* **1999**, *111*, 448−468.

(4) (a) Collins, S.; Ward, D. G. *J. Am. Chem. Soc.* **1992**, *114*, 5460−5462. (b) Collins, S.; Ward, D. G.; Suddaby, K. H. *Macromolecules* **1994**, *27*, 7222−7224. (c) Collins, S.; Li, Y.; Ward, D. G.; Reddy, S. S. *Macromolecules* **1997**, *30*, 1875−1883.

(5) (a) Stuhldreier, T. Polymerisation von Methylmethacrylat, Methylacrylat and α,β-ungesältigten Lactonen mit Zirconocenkatalysateren. Dissertation, RWTH Aachen, 1999 (in German). (b) Stuhldreier, T.; Keul, H.; Höcker, H. *Macromol. Rapid Commun.* **2000**, *21*, 1093−1098.

(6) (a) Hatada, K.; Kitayama, T.; Ute, K.; Nishiura, T. *Macromol. Symp.* **1993**, *70/71*, 57−66. (b) Hatada, K.; Kitayama, T.; Ute, K. *Macromol. Symp.* **1998**, *132*, 221−230. (c) Hatada, K. *J. Polym. Sci., Part A: Chem.* **1999**, *37*, 245−260.

(7) (a) Yasuda, H.; Yamamoto, H.; Yokota, K.; Miyake, S.; Nakamura, A. *J. Am. Chem. Soc.* **1992**, *114*, 4908−4910. (b) Yasuda, H.; Yamamoto, H.; Yamashita, M.; Yokota, K.; Nakamura, A.; Miyake, S.; Kai, Y.; Kanehisa, N. *Macromolecules* **1993**, *26*, 7134−7143. (c) Yasuda, H.; Ihara, E. *Macromol. Chem. Phys.* **1995**, *196*, 2417−2441. (d) Ihara, E.; Morimoto, M.; Yasuda, H. *Macromolecules* **1995**, *28*, 7886−7892. (e) Giardello, M. A.; Yamamoto, Y.; Brard, L.; Marks, T. J. *J. Am. Chem. Soc.* **1995**, *117*, 3276−3277. (f) Desurmont, G.; Li, Y.; Yasuda, H.; Maruo, T.; Kanehisa, N.; Kai, Y. *Organometallics* **2000**, *19*, 1811−1813.

(8) (a) Deng, H.; Shiono, T.; Soga, K. *Macromolecules* **1995**, *28*, 3067−3073. (b) Saegusa, N.; Saito, T.; Shiono, T.; Ikeda, T.; Deng, H.; Soga, K. In *Metalorganic Catalysts for Synthesis and Polymerization*; Kaminsky, W., Ed.; Springer-Verlag: Berlin, 1999; pp 583−589.

(9) Nguyen, H.; Jarvis, A. P.; Lesley, M. J. G.; Kelly, W. M.; Reddy, S. S.; Taylor, N. J.; Collins, S. *Macromolecules* **2000**, *33*, 1508−1510.

(10) (a) Cameron, P. A.; Gibson, V. C.; Graham, A. J. *Macromolecules* **2000**, *33*, 4329−4335. (b) Cameron, P. A.; Gibson, V. C.; Irvine, D. J. *Angew. Chem.* **2000**, *112*, 2225−2228.

(11) Frauenrath, H. Polymerization of olefins and functionalized monomers with zirconocene catalysts. Dissertation, RWTH Aachen, 2001 (in English).

(12) Sustmann, R.; Sicking, W.; Bandermann, F.; Ferenz, M. *Macromolecules* **1999**, *32*, 4204−4213.

(13) (a) Shaltout, R. M.; Corey, J. Y.; Path, N. R. *J. Organomet. Chem.* **1995**, *503*, 205−212. (b) Corey, J. Y.; Zhu, X.-H.; Brammer, L.; Path, N. P. *Acta Crystallogr., Sect. C* **1995**, *51*, 565−567. (c) Bajgur, C. S.; Tikkanen, W. R.; Petersen, J. L. *Inorg. Chem.* **1985**, *24*, 2539−2546.

(14) Amorose, D. M.; Lee, R. A.; Petersen, J. L. *Organometallics* **1991**, *10*, 2191−2198.

MA001251V